Kaluza-Klein structure associated with a fat brane

Pham Quang Hung* and Ngoc-Khanh Tran†
Department of Physics, University of Virginia, 382 McCormick Road, Charlottesville, Virginia 22904-4714, USA
(Received 30 September 2003; published 4 March 2004)

It is known that the imposition of orbifold boundary conditions on a background scalar field can give rise to a nontrivial vacuum expectation value along extra dimensions, which in turn generates fat branes and associated unconventional Kaluza-Klein (KK) towers of fermions. We study the structure of these KK towers in the limit of one large extra dimension and show that normalizable (bound) states of massless and massive fermions can exist at both orbifold fixed points. A closer look, however, indicates that orbifold boundary conditions act to suppress at least half of the bound KK modes, while periodic boundary conditions tend to drive high-lying modes to a conventional structure. By investigating the scattering of fermions on branes, we analytically compute the masses and wave functions of KK spectra in the presence of these boundary conditions up to the one-loop level. The implication of KK-number nonconservation couplings for the Coulomb potential is also examined.

DOI: 10.1103/PhysRevD.69.064003 PACS number(s): 04.50.+h, 11.25.Mj

I. INTRODUCTION

Conventionally, Kaluza-Klein (KK) towers of modes arise from the compactification of extra dimensions, i.e., the imposition of periodic boundary conditions on those finite extra dimensions, to render effectively the low-energy 4D physics from a bigger spacetime with finite spatial extra dimensions (see, e.g., [1]). Given that the standard model (SM) is the standard low-energy effective theory of particle interaction, one requires that any higher-dimensional scenario reduces to the SM at the electroweak scale. From the KK perspective, this requires the lowest modes in KK towers of fermions to be chiral because these are the only ones we observe at low energy. To this end, the simple periodic compactification needs to be replaced by an orbifold compactification and, in the case of one extra dimension, the common choice is S^1/Z_2 compactification.

A novel mechanism has been proposed to localize standard model chiral fermions differently along extra dimensions making use of the Yukawa interaction of these fields with a background scalar field [2] (see also [3]). This approach is phenomenologically very attractive, because it allows for easy control of the 4D effective couplings by regulating the overlap of particle wave functions in the extra dimensions. At the core of this mechanism, the necessary background scalar field of a nontrivial vacuum expectation value (VEV) profile along the extra dimension has been explicitly realized through the imposition of various orbifold boundary conditions [4] (see also [5]). Because of the nature of this mechanism, one sees that the KK modes obtained are intimately related to the structure of this scalar VEV in the transverse direction. At the same time, as in theories with finite extra dimensions, the usual periodic boundary conditions (i.e., periodic compactification) certainly drive KK towers back to the conventional structure. It is then of interest to analyze in detail the interplay between these two tendencies revealed in the KK structure of related fields.

For this purpose, we find it particularly useful to treat the dependence of fields on the extra dimensions as wave functions subject to the potential along the extra dimension associated with the background scalar kink solution (or ''bulk potential'' in short), whose centers are located at fixed points of the orbifold. In what follows, these defects will be referred to as fat branes. In this view, we find that in the limit of a large extra dimension, bound (i.e., normalizable) KK states of massive fermions can actually exist at both fixed points, because the bulk potential possesses local minima (or ''potential wells'') at those points (see Fig. 2 below). This differs from the conclusion of [4], where in the same limit of a large extra dimension, normalizable KK states are found only at one of the fixed points. This approach further allows us to make a direct connection between the boundary conditions imposed on the wave functions and the transmission amplitude in the related scattering process of particles on the branes.

Our presentation is structured as follows. Section II reviews the fermion localization mechanism [4,2] in a model with one infinite extra dimension, where the extra dimensional wave function of the fields and the corresponding KK mass can be exactly determined from the bulk potential viewpoint. In this limit, the periodic boundary conditions (PBCs) do not exist, so very distinct KK towers, partially discretized, originating from orbifold boundary conditions (OBCs) can readily be seen. Section III generalizes the calculation to the case of a large, but finite, extra dimension. Here the competition between the two types of boundary conditions becomes apparent. We show that, in this limit the OBCs essentially require wave functions along the extra dimension of any single KK mode to have the same parity at all fixed points, whereas bulk potentials tend to make them different at these points (see Fig. 2). As a result, this parity mismatch strongly affects KK light modes, while for the heavier KK modes, the same boundary conditions can be equivalently translated into the requirement that these KK fermions cross the branes without reflection. Hence, in all cases, OBCs generally suppress many bound and low-lying

*Electronic address: pqh@virginia.edu
†Electronic address: nt6b@virginia.edu

KK modes. Section IV will highlight the fact that symmetry breaking effects in the transverse dimension are actually encoded in the effective couplings, which in turn generate nonuniversal and KK-number nonconservating interaction vertices of fermion–gauge boson and fermion-scalar. Sections IV A and IV B examine the implication of these effects for the Coulomb potential and the one-loop correction to the KK masses, respectively, from a 4D effective viewpoint. In a different but related problem and in order to clarify the physical meaning of the KK mass equation obtained in orbifold compactification, Sec. V studies the scattering of fermion on branes. It is found that low-lying KK modes of the fermion indeed survive only when resonant transmission through the branes occurs, which in turn is achieved only for some very particular values of the brane's parameters. Section VI summarizes our main results and offers some outlook. The Appendix classifies properties of the general solutions of a hypergeometric-related differential equation encountered throughout the paper.

II. FERMION LOCALIZATION IN EXTRA DIMENSIONS

Consider the case of a massless fermion and a real scalar field in $4+1$ dimensions. We use y to denote the fifth dimension's coordinate, $y\in[0,L]$. In this section we will eventually let $L\to\infty$. The Lagrangians

$$\mathcal{L}_\psi=\overline{\psi}(x,y)[i\gamma^\mu\partial_\mu-\gamma^5\partial_y-f\phi(x,y)]\psi(x,y), \tag{1}$$

$$\mathcal{L}_\phi=\frac{1}{2}\partial^\mu\phi(x,y)\partial_\mu\phi(x,y)-\frac{1}{2}\partial_y\phi(x,y)\partial_y\phi(x,y) - \frac{\lambda}{4}[\phi^2(x,y)-v^2]^2, \tag{2}$$

$$\mathcal{L}=\mathcal{L}_\psi+\mathcal{L}_\phi \tag{3}$$

are invariant under Z_2 symmetry

$$\phi(x,y)\to\Phi(x,y)\equiv-\phi(x,L-y), \tag{4}$$

$$\psi(x,y)\to\Psi(x,y)\equiv\gamma_5\psi(x,L-y), \tag{5}$$

which in turn allows the imposition of the following orbifold and periodic boundary conditions:

$$\phi(x,-y)=\Phi(x,L-y)=\phi(x,2L-y), \tag{6}$$

$$\psi(x,-y)=\Psi(x,L-y)=\psi(x,2L-y). \tag{7}$$

We note that all fields are $2L$ periodic and the imposition of these boundary conditions actually transforms the extra dimension into an orbifold S^1/Z_2 with two fixed points at $y=0$ and $y=L$. As $\phi(y)$ is antisymmetric at these points, if λv^2 is sufficiently large, the minimization of effective potential

$$V(\phi)=\frac{1}{2}\partial_y\phi(x,y)\partial_y\phi(x,y)+\frac{\lambda}{4}[\phi^2(x,y)-v^2]^2 \tag{8}$$

gives rise to a kink solution of the VEV in the bulk (in the limit $L\to\infty$)

$$\langle\phi(x,y)\rangle=h(y)=v\tanh\sqrt{\frac{\lambda v^2}{2}}y. \tag{9}$$

By performing a chiral decomposition

$$\psi(x,y)=\psi_R(x)\xi_R(y)+\psi_L(x)\xi_L(y) \tag{10}$$

where the functions[1] $\xi_{R,L}$ satisfy the OBCs (7),

$$\xi_{R,L}(-y)=\pm\xi_{R,L}(y),\quad \xi_{R,L}(L-y)=\pm\xi_{R,L}(L+y), \tag{11}$$

we obtain the equations of motion for 4D chiral fields:

$$i(\gamma^\mu\partial_\mu\psi_L)\xi_L-\psi_R(\partial_y+fh)\xi_R=0,$$

$$i(\gamma^\mu\partial_\mu\psi_R)\xi_R-\psi_L(-\partial_y+fh)\xi_L=0. \tag{12}$$

The 4D Dirac mass can be explicitly recovered when we take $\xi_{R,L}\to\xi_{mR,L}$ with [4,2]

$$(\partial_y+fh)\xi_{mR}=m\xi_{mL},\quad (-\partial_y+fh)\xi_{mL}=m\xi_{mR}. \tag{13}$$

As usual, when $m\neq0$, these equations are coupled and we can combine them to make a second-order differential equation for each of ξ_R and ξ_L. Once ξ_R (and m) is obtained, one can put it back into Eq. (13) to solve for ξ_L (see the Appendix). But here, for the purpose of visualizing ξ_R,ξ_L as wave functions subject to different "bulk potentials" $V_R^{(1)},V_L^{(1)}$, we choose to work equally with both second-order equations as shown below

$$[-\partial_y^2+V_R^{(1)}(y)]\xi_{mR}=m^2\xi_{mR},$$

$$[-\partial_y^2+V_L^{(1)}(y)]\xi_{mL}=m^2\xi_{mL}, \tag{14}$$

where we have defined by virtue of Eq. (9)

$$w\equiv fv,\quad u\equiv\sqrt{\frac{\lambda v^2}{2}},$$

$$V_{R,L}^{(1)}(y)\equiv\mp uw\frac{1}{\cosh^2uy}+w^2\tanh^2uy. \tag{15}$$

In this "Schrödinger-like equation," evidently $\xi_{mR,L}$ and the squared KK mass m^2 are, respectively, the eigenstates and eigenvalues subject to an analogue quantum-mechanical problem. The width of the underlying "potential wells" is $\sim1/u\sim\sqrt{1/\lambda v^2}$ and is the actual thickness of the domain wall (or fat brane) separating domains of different asymptotic values of scalar VEV along the fifth dimension. From Fig. 1 we see that, if $u\geqslant w$, then $V_L^{(1)}$ becomes a "po-

[1]The decomposition (10) requires that $\xi_{R,L}(y)$ be continuous functions because they represent the probability amplitude of finding fermions in the extra dimension.

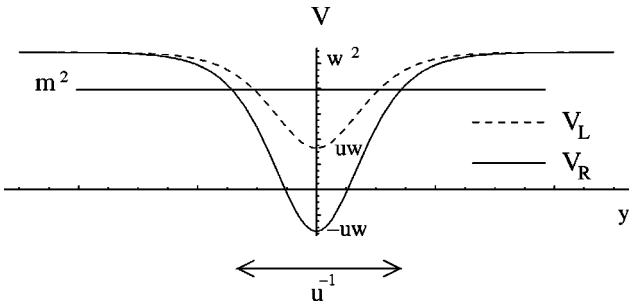

FIG. 1. Potentials $V^{(1)}_{R,L}$ experienced by fermions in the limit $L \to \infty$.

tential hump'' and it possesses no bound states; thus for the sake of completeness, in the rest of this work we assume that u is essentially smaller than w. Equations (14) are related to hypergeometric differential equation and can be exactly solved [6].

In the lower part of the spectrum ($m^2 < w^2$), bound KK masses are necessarily quantized, and their exact values can be obtained as [see Eqs. (A1), (A10), (A25) of the Appendix]

$$m_n^2 = 2n_R uw - n_R^2 u^2 \quad \left(0 \leqslant n_R < \frac{w}{u}\right), \tag{16}$$

$$m_n^2 = 2(n_L+1)uw - (n_L+1)^2 u^2 \quad \left(0 \leqslant n_L < \frac{w}{u} - 1\right), \tag{17}$$

where the ranges on $n_{R,L} \in N$ come from the constraints $m^2 < w^2$, $m_n \geqslant 0$. The corresponding eigenfunctions can be written in terms of hypergeometric functions and are given in Eqs. (A9), (A23). The parity constraints (11) on these wave functions further require n_R and n_L to be even and odd integers, respectively. The KK masses (16), (17) are already surprising as they indicate that the mass gap of the KK spectrum is finite even when the bulk volume is infinite ($L \to \infty$). Indeed the KK spectrum is discretized for the first few levels ($n < w/u$) because the whole spectrum has been spontaneously distorted by nontrivial VEVs through Yukawa interaction. In other words, the KK spectrum is now associated with the internal structure of the fat brane, and not solely with the compactification.

In this bulk potential picture, for the zero mode $m_n = 0$, we have $n_R = 0$ and no satisfying value of n_L, because (see Fig. 1) the $m_n^2 = 0$ level is even lower than the lower limit of the potential $V_L^{(1)}$, so only the right-handed zero mode is normalizable and survives.[2] This eventually can be identified with the standard model chiral fermions. Various interesting phenomenological applications of fat brane models, such as the fermion mass hierarchy, *CP* violation, baryogenesis, and proton decay suppression, etc., have been carried out in numerous works (see, e.g., [2,5,7]).

[2]By flipping the sign of γ_5 in Eq. (5), one can invert the situation where now only the left-handed zero mode survives.

The nonzero KK modes of mass m_n come in pairs of both chiralities with the relation (16), (17)

$$n_R = n_L + 1. \tag{18}$$

Obviously, this assures the difference in parity of $\xi_{R,L}$ as earlier required by the OBCs. In the case that L is finite, the relation (18) is so strict that it apparently acts to suppress many light KK modes as we will see in the next section.

We now proceed to the continuous spectrum $m^2 \geqslant w^2$, $k \equiv \sqrt{(m^2 - w^2)/u^2}$. With the parity constraints (11) we can unambiguously construct the corresponding wave functions [see Eqs. (A19), (A32)], whose asymptotic forms are

$$y \to \pm\infty:\ \xi_{mR}(y) \to 2^{-ik}\left(e^{\pm ikuy} + \frac{D_1}{1-D_2} e^{\mp ikuy}\right), \tag{19}$$

$$y \to \pm\infty:\ \xi_{mL}(y) \to \pm 2^{-ik}\left(e^{\pm ikuy} - \frac{D_1'}{1+D_2'} e^{\mp ikuy}\right), \tag{20}$$

where D_1, D_2, D_1', D_2' are given in Eqs. (A17), (A30). Manifestly, ξ_{mR} and ξ_{mL} are symmetric and antisymmetric functions under $y \to -y$ at $y = 0$. However, in Eqs. (19), (20) we also see that matter waves propagate in both directions even as $y \to \pm\infty$, signaling the existence of other fixed points at infinity, from which waves reflect. But in the limit $L \to \infty$ considered here, this reflection does not seem to be very reasonable. Either way, this is not more problematic, because the model of the infinite extra dimension itself is not realistic as soon as we introduce gauge fields that can propagate in the bulk. For now we just note that the reflection from infinity is a consequence of the orbifold boundary condition (7) imposed on the fermion fields. The next sections will discuss the more realistic case of finite L.

Similarly, one can analyze the KK expansion of background scalar field $\phi(x,y)$ about its VEV $h(y)$ [4]:

$$\phi(x,y) = h(y) + \sum_n \phi_n(x) f_n(y) \tag{21}$$

with $f_n(y)$ being antisymmetric at both fixed points. As before, the 4D Klein-Gordon mass of KK scalar modes ϕ_n is recovered when f_n satisfies

$$[-\partial_y^2 + \Delta^2(y)] f_n(y) = \overline{m_n^2} f_n(y), \tag{22}$$

where in the limit $L \to \infty$

$$\Delta^2(y) = \lambda v^2 (3\tanh^2 uy - 1). \tag{23}$$

The general solutions of Eq. (22) are given in the Appendix. We find that, for the discrete spectrum, $\overline{\varepsilon} \equiv \sqrt{(4u^2 - \overline{m^2})/u^2} > 0$, there is only one bound eigenstate antisymmetric at $y = 0$ (A33) of quantum numbers (A34) $\overline{n} = 1$, $\overline{\varepsilon} = 1$,

$$f(y)=\frac{1}{\cosh uy}F\left(-1,4,2;\frac{1}{1+e^{2uy}}\right)=\frac{\tanh uy}{\cosh uy} \quad (24)$$

corresponding to the KK mass $\bar{m}=\sqrt{3}u$.

For the continuous spectrum, $\bar{m}^2\geqslant 4u^2$, $\bar{k}\equiv\sqrt{(\bar{m}^2-4u^2)/u^2}=i\bar{\varepsilon}$, the wave function $f_n(y)$ being antisymmetric at $y=0$ can be found [see Eq. (A40)]. Its asymptotic form is

$$y\to\pm\infty:$$

$$f_n(y)\to\pm 2^{-i\bar{k}}\left(e^{\pm i\bar{k}uy}-\frac{\Gamma(-i\bar{k})\Gamma(1-i\bar{k})}{\Gamma(-i\bar{k}-2)\Gamma(-i\bar{k}+3)}e^{\mp i\bar{k}wy}\right) \quad (25)$$

where $\bar{D}$ is given in Eq. (A41). This shows that, just as in the case of the fermion described below Eq. (20), the orbifold boundary condition (6) gives rise to the nonphysical reflection from infinity of background scalar wave functions in the extra dimension. This point will be clarified below in a more realistic scenario where the other orbifold fixed point is taken into account by considering large, but not infinite L.

III. FINITE LIMIT OF EXTRA DIMENSION

In the model of an infinite and flat extra dimension investigated in the last section, the KK masses and wave functions can be solved exactly, but it may not be realistic as soon as the SM gauge bosons or graviton are introduced.[3] In this section we consider a more realistic situation where L is finite and much larger than the thickness of branes ($L\gg\sqrt{2/\lambda v^2}=1/u$). In this limit, the VEV of the background scalar field satisfying the OBCs (6) is given approximately by [4]

$$h(y)=v\tanh\left(\sqrt{\frac{\lambda v^2}{2}}y\right)\tanh\left(\sqrt{\frac{\lambda v^2}{2}}(L-y)\right)+\mathcal{O}(e^{-L\sqrt{\lambda v^2}}). \quad (26)$$

From this one obtains

$$[-\partial_y^2+V_R^{(2)}(y)]\xi_{mR}=m^2\xi_{mR},$$
$$[-\partial_y^2+V_L^{(2)}(y)]\xi_{mL}=m^2\xi_{mL}, \quad (27)$$

with new composite potentials

$$V_{R,L}^{(2)}(y)=\mp uw\left(\frac{\tanh u(L-y)}{\cosh^2 uy}-\frac{\tanh uy}{\cosh^2 u(L-y)}\right)+w^2\tanh^2 uy\tanh^2 u(L-y). \quad (28)$$

In Fig. 2 we sketch the potential (28) for the case $L=10\sqrt{2/\lambda v^2}$. It is clear that, in the limit $L\gg 1/u$, each new potential ($V_R^{(2)}$ or $V_L^{(2)}$) has the shape of a neatly separated double-well potential, whose component wells are just of the forms (15). More specifically, the new $V_R^{(2)}$ (28) looks exactly like $V_R^{(1)}$ [of (15)] at the fixed point $y=0$, and like $V_L^{(1)}$ at $y=L$. The opposite holds for $V_L^{(2)}$. Consequently, the new composite wave functions [solutions of (27)] can be obtained by matching together the solutions of Eq. (14) found earlier.

For light (bound) KK modes, $m^2<w^2$, $\varepsilon\equiv\sqrt{(w^2-m^2)/u^2}>0$, the matching appears straightforward since the wave functions given by Eqs. (A9), (A23) tend to zero at the matching region $y\simeq L/2$ [see Eqs. (A7), (A24)]. However, there exists a subtlety in the parity matching due to the shape interchange of $V_R^{(2)}$ and $V_L^{(2)}$ at the fixed points, as we mentioned above. At the same squared mass level m^2, ξ_{mR} behaves like a right-handed wave function at $y=0$ and a left-handed wave function at $y=L$, so in view of Eq. (11), if ξ_{mR} is symmetric at $y=0$, it must be antisymmetric at $y=L$, or vice versa. Meanwhile the OBCs (11) also require ξ_{mR} to be symmetric at all fixed points. So if ξ_{mR} were a solution satisfying these apparently contradictory conditions on parity and were nonzero in the vicinity of $y=0$, then it should be zero around $y=L$, because a null function is the only function that is both symmetric and antisymmetric with respect to a given point. A similar parity mismatch also holds for left-handed states. As a result, we find that (Fig. 2) the tower of bound KK states with mode indices $n=0,2,\ldots$ will be localized at $y=0$, while the tower with $n=1,3,\ldots$ is localized at $y=L$ with n being defined in Eq. (16). All these modes are vectorlike (i.e., they possess both right- and left-handed components), except for the zero mode being right-handed localized at $y=0$.[4] These towers do not essentially correlate, but in the limit $L\sim 1/u$ stronger tunneling may change the qualitative picture.

We can see this more clearly now by studying the upper part of the spectrum, where $m^2\geqslant w^2$, $k\equiv\sqrt{(m^2-w^2)/u^2}=i\varepsilon$. Here the matching process is simple, because as noted earlier, at the matching region in between the two wells, the wave functions associated with each well already fully reach their asymptotic forms. Using Eqs. (A19) and (A31) [or Eqs. (A20) and (A32)], the matching induces the following relation:

$$\frac{D_1}{1-D_2}=e^{2ikuL}\frac{1-D_2'}{D_1'} \quad (29)$$

[3]Theories with infinite but warped extra dimensions effectively consistent with 4D physics have been built (see [8]).

[4]In [4], after combining Eqs. (13) and (26) to get the zero-mode wave function $\xi_{0R}=\mathcal{C}[\cosh u(L-y)]^{v/u}\sim e^{fv(L-y)}$ close to the fixed point $y=L$, it is accordingly found that the zero and other massive KK modes are non-normalizable at $y=L$. Although ξ_{0R} increases exponentially as y runs away from $y=L$, we think that the matching of this function with the zero-mode state (A9) bound to the fixed point $y=0$, which decreases exponentially into the bulk, would necessarily set the constant $\mathcal{C}$ to zero in order to preserve the normalization of ξ_{0R} in the limit of large L. As a result, the right-handed zero mode exists only around $y=0$ while certain higher normalizable modes can exist around both fixed points as seen in the bulk potential picture (Fig. 2).

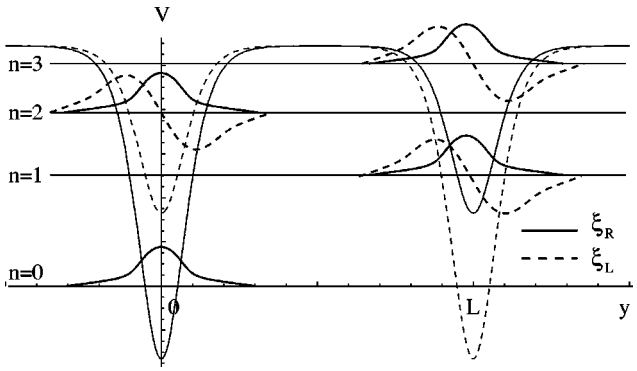

FIG. 2. Potentials $V^{(2)}_{R,L}$ and symbolic wave functions $\xi_{R,L}$ of fermion chiral components with $L=10/u$. The solid curves represent $V^{(2)}_R$ and its symmetric wave functions ξ_R, the dashed curves represent $V^{(2)}_L$ and the antisymmetric ξ_L.

where D and D' are given in Eqs. (A17), (A30). Since all wave functions are 2L periodic [Eq. (7)], we can rewrite Eq. (29) as

$$e^{2ikuL}=1\Leftrightarrow ku=\frac{n\pi}{L}, \tag{30}$$

$$D_1D_1'+D_2^2=1. \tag{31}$$

The first of these equations is the usual periodic boundary conditions, while the second accounts for orbifold boundary conditions and the effect of fat branes. Because k, D's are all functions of m, Eqs. (30), (31) are actually equations determining the KK masses.

Remarkably, the physical meaning of condition (31) can be viewed as the requirement that the transmission amplitude of fermions in the double-brane system needs to be exactly 1. A quantitative discussion will be given in Sec. V. However, the assertion's outcome itself is readily plausible: once the transmission amplitude is 1, the KK states propagate in the bulk as if there were no potential at all, and subsequently the periodic boundary condition (30) drives them to the conventional structure. As a result, we expect high-lying modes of the KK spectrum to have a structure closer to that of periodic compactification.

Let us now examine the compatibility of the two conditions (30), (31). For very heavy KK modes ($k\gg w/u>1$), D_1, D_1' and D_2, D_2' approach 1 and zero, respectively, and the condition (31) is automatically satisfied. Then Eq. (30) implies $m^2=w^2+k^2u^2=w^2+n^2\pi^2/L^2\approx n^2\pi^2/L^2$, which is the usual KK mass from periodic compactification. For smaller values of k, it may be difficult to solve Eq. (31) analytically although a numerical approach is possible. In Sec. V we will discuss the solution of this equation in the limit of small k. Here we just mention that for a k that is not very large the two conditions (30), (31) are not always compatible. To illustrate this point, let us consider the special case where $s\equiv w/u$ is an integer. Using $\Gamma(z+1)=z\Gamma(z)$ and Eq. (A18), we find $D_2=D_2'=0$ and

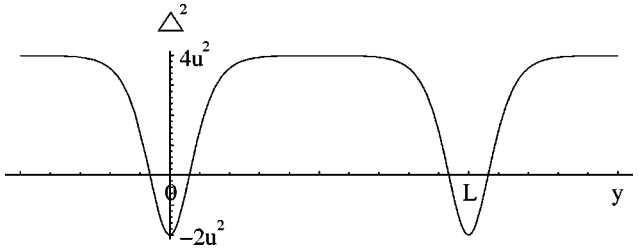

FIG. 3. Potentials $\Delta^2(y)$ experienced by scalar fields with $L=10/u$.

$$D_1=\frac{(ik+1)\cdots(ik+s)}{(ik-1)\cdots(ik-s)},\quad D_1'=\frac{(ik+1)\cdots(ik+s-1)}{(ik-1)\cdots(ik-s+1)}. \tag{32}$$

Equation (31) becomes a polynomial equation of order $(k^2)^{s-1}$, so it has at most $(s-1)$ solutions of k^2 (or squared mass m^2), which may or may not satisfy Eq. (30). In any case, the combination of Eqs. (30), (31) gives no more than $(s-1)$ different exact values of m^2 in the range of not-too-large k ($k\leqslant s\equiv w/u$), while in the conventional compactification (30) the number of KK states in the same range is $\sim wL/\pi\gg 1$.[5] Combined with the earlier consideration for bound KK states, we see clearly that the lower part of the KK spectrum is strongly distorted by spontaneous breaking of the background scalar, to which the fermions are coupled, and also by orbifold boundary conditions, and the latter are generally so strict that many of these states are effectively suppressed. The higher levels are not essentially affected by the bulk potential (their transmission coefficient is close to unity), and the usual periodic boundary conditions drive their mass structure to that of conventional compactification.

We now briefly investigate the KK scalar structure (21), (22) in the limit $L\gg 1/u$ by a similar method. In this limit, the potential (23) becomes [see Eq. (26)]

$$\Delta^2(y)=\lambda v^2[3\tanh^2 uy\tanh^2 u(L-y)-1]. \tag{33}$$

This potential is sketched in Fig. 3 for $L=10/u=10\sqrt{2/\lambda v^2}$. We see that the two component wells are identical (i.e., the potential is L periodic) and no parity mismatch occurs, and we still have only one antisymmetric KK state (24) with mass $\bar{m}=\sqrt{3}u$ in the lower part of the spectrum. For the higher modes $\bar{m}^2\geqslant 4u^2$, the matching of the scalar wave functions $f(y)$ [Eq. (A40)] antisymmetric at all fixed points generates the following relations:

$$\bar{k}u=\frac{\bar{n}\pi}{L}, \tag{34}$$

$$\bar{D}^2=\left(\frac{(1+i\bar{k})(2+i\bar{k})}{(1-i\bar{k})(2-i\bar{k})}\right)^2=1, \tag{35}$$

[5]However, we will see later that the case of the integral w/u is a special "resonant" case, where Eq. (31) is approximately satisfied for very small values of k.

where $\bar{k}\equiv\sqrt{(\bar{m}^2-4u^2)/u^2}$. These equations have at most two exact solutions $\bar{k}^2=0$ and $\bar{k}^2=2$ (the latter is a true solution if only $\sqrt{2}Lu/\pi$ is integer) corresponding to $\bar{m}^2=4u^2$ and $6u^2$. However, for all $\bar{k}\ll 1$ or $\bar{k}\gg 1$, the condition (35) is approximately satisfied and in these ranges only the periodic boundary condition (34) effectively governs the KK masses and gives them the conventional structure up to a constant shift:

$$\bar{m}_n^2=u^2(4+\bar{k}^2)=u^2\left(4+\frac{\bar{n}^2\pi^2}{u^2L^2}\right), \tag{36}$$

where $\bar{n}\gg uL/\pi$ or $\bar{n}\ll uL/\pi$. As scalars are not chiral, they do not suffer from parity mismatch and consequently their transmission coefficient can reach unity not only for high-lying KK levels, but also for levels immediately above the surface of the potential well. This ''resonant behavior'' of the potential (23) was discovered a long time ago (see [9]). We note that, in contrast with the result obtained therein, here the scalar fields are constrained to be antisymmetric by OBCs, and then resonance occurs only in the two above ranges of momentum $\bar{k}$. This special structure of the KK scalar spectrum has important implications in practical calculations, as we will see in the following fermion self-energy evaluation.

IV. FOUR-DIMENSIONAL EFFECTIVE COUPLINGS AND IMPLICATIONS

It is well known that in the universal extra dimension (UED) scenario (see, e.g., [10]) where no localization mechanism is invoked and all extra dimensions are accessible to all fields, momentum is conserved in both the longitudinal (infinite) and transverse (finite) directions of space. This in turn implies the KK-number conservation of all vertex interactions, and there are no tree-level contributions from KK excitation to standard model observables, whose content fields are taken to be the zero modes in the KK tower picture. The situation is quite different in the brane scenario, where Lorentz invariance is violated along transverse dimensions due to both the background kink and orbifold compactification. Consequently, in the reduced 4D picture, there exist KK-number nonconservation vertices characterized by effective couplings. This is because the overlap integral over extra coordinates leading to 4D couplings actually measures the effects of Lorentz invariance breaking on the wave functions of related fields along the extra dimension. These couplings may give rise to new interesting phenomenologies such as tree-level flavor changing neutral currents, new mixing of quark and lepton flavors, etc. The comparison of these new contributions with experimental data will provide bounds on various parameters of the model. In this section, just for the purpose of illustration, we will present a toy model which involves only one fermion flavor in order to study the new implications, if any, of the brane scenario for the Coulomb interaction in a tree-level consideration and for the KK masses up to one-loop level.

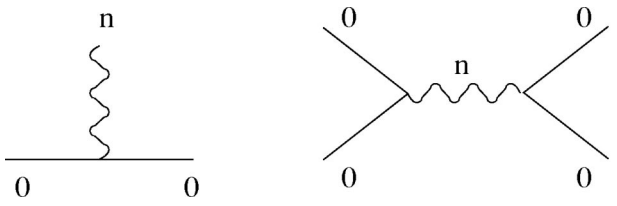

FIG. 4. Effective fermion-photon vertex and tree-level fermion scattering diagram.

A. Static Coulomb interaction

Charged fermions in QED interact with one another by exchanging a photon. We now assume that the photon can propagate freely along the fifth dimension, otherwise a localization mechanism for the gauge boson in exact fashion such as we used for fermions encounters a serious complication related to the issue of universality of charge. The S^1/Z_2 OBCs turn the extra dimensional wave function of the photon KK modes into the form of cosine or sine functions depending on their transformation property under Z_2. The Z_2 symmetry of the term $\bar{\psi}\gamma^M A_M\psi$ requires the photon's first four components A_μ to be symmetric and the fifth A_5 antisymmetric at $y=0,L$. This also eliminates the zero mode of A_5 as well as the contribution of its KK excitations A_{n5} to the zero-mode charged fermions interaction (Fig. 4). After dimensional reduction, we obtain the following vertex coupling of the fermion zero mode and photon KK modes:

$$\begin{aligned}\int dy\,\bar{\psi}(x,y)[-e_5\not{A}(x,y)]\psi(x,y)\\ \rightarrow -e\bar{\psi}_0(x)\gamma^\mu A_{0\mu}(x)\psi_0(x)\\ -\sum_{n=1}^{\infty}\epsilon_n\bar{\psi}_0(x)\gamma^\mu A_{n\mu}(x)\psi_0(x)\end{aligned} \tag{37}$$

where the ϵ_n's are 4D effective couplings

$$\epsilon_n\equiv\frac{e_5}{\sqrt{L}}\int_0^{2L}dy[\xi_0(y)]^2\cos\left(\frac{n\pi y}{L}\right) \tag{38}$$

and $e=e_5/\sqrt{2L}$ is the usual 4D charge of the fermion zero mode, whose wave function is $\xi_0(y)=(\cosh uy)^{-w/u}$ as given in Eq. (A9). In the nonrelativistic limit, the potential between two charged fermion zero modes can be found by working out the KK photon exchange process depicted in Fig. 4. The result is

$$V(r)=\frac{e^2}{r}+\sum_{n=1}^{\infty}\frac{\epsilon_n^2}{r}e^{-n\pi r/L}$$
$$=\frac{e^2}{r}+\frac{2e^2}{r}\int_0^{2L}dy[\xi_0(y)]^2\int_0^{2L}dy'[\xi_0(y')]^2$$
$$\times\sum_{n=1}^{\infty}\cos\left(\frac{n\pi y}{L}\right)\cos\left(\frac{n\pi y'}{L}\right)e^{-n\pi r/L} \quad (39)$$

where r denotes the spatial separation in the 4D picture. The first term of Eq. (39) represents the contribution of the massless photon, while the remaining terms come from its massive KK modes. By transforming the sum over the mode index n into a sum over elements of a geometric series, and approximating $\xi_0(y)$ with a Gaussian function (A11), we obtain the following expression for the potential $V(r)$:

$$V(r)=\frac{e^2}{r}+\frac{2e^2}{r}\left[-1+\frac{1}{1-e^{-\pi r/L}}\right.$$
$$\left.-\frac{3\pi^2}{4wuL^2}\frac{e^{-\pi r/L}(1+e^{-\pi r/L})}{(1-e^{-\pi r/L})^3}+\mathcal{O}\left(\frac{1}{w^2u^2L^4}\right)\left(\frac{L}{r}\right)^5\right]. \quad (40)$$

If $r\gg L$ (and $r>1/M_Z$ so that the contribution from the Z boson can be neglected), the potential (40) takes the form

$$V(r)\simeq\frac{e^2}{r}+\left(1-\frac{3\pi^2}{4wuL^2}\right)\frac{2e^2}{r}e^{-\pi r/L}+\cdots, \quad (41)$$

where we have kept only a few terms of higher orders. The first term in Eq. (41) is the usual Coulomb interaction potential arising from the exchange of the zero mode of the photon, whereas the second term has a Yukawa potential form because it is mediated by an infinite tower of massive KK modes. This correction is considerable only when r approaches the size of the extra dimension, and the brane's explicit contribution to this correction is at most a few percent in the limit $L\gg u$, so it is unlikely that we could find some phenomenological bounds on the model's parameters u and w by just looking at the static Coulomb interaction potential.[6]

B. One-loop correction to KK mass

It is known that in theories with just one extra dimension the sum over an infinite tower of KK modes for tree-level diagrams converges as we have seen above. At the loop levels this is no longer true and some renormalization procedure is needed. To see specifically how the KK-number nonconservating couplings contribute in an actual loop computation, let us evaluate, as an example, the fermion self-energy at one loop and its corresponding mass shift in the 4D effective picture.

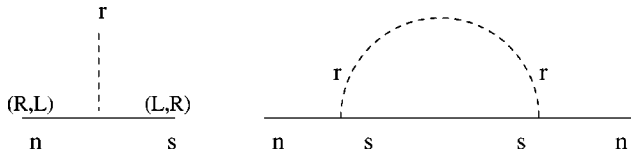

FIG. 5. Effective fermion-scalar vertex and fermion self-energy diagram.

Decomposing $\psi(x,y)$ and $\phi(x,y)$ as in Eqs. (10), (21) and performing the integration over the y coordinate we transform the Lagrangian $\mathcal{L}_\psi(1)$ into its 4D version:

$$\int\mathcal{L}_\psi dy=\sum_n\bar{\psi}_n(x)(\not{\partial}-m_n)\psi_n(x)-\sum_{n,r,s}f\bar{\psi}_n(x)\phi_r(x)$$
$$\times(g_{RL}^{nrs}P_L+g_{LR}^{nrs}P_R)\psi_s(x),$$

where the m_n's are the tree-level masses of KK fermions and the g's are the effective 4D couplings (Fig. 5):

$$g_{RL}^{nrs}=\int\xi_{nR}(y)f_r(y)\xi_{sL}dy,\quad g_{LR}^{nrs}=\int\xi_{nL}(y)f_r(y)\xi_{sR}dy. \quad (42)$$

We note that in g_{RL}^{nrs} the OBCs require n and s to be even and odd integers, respectively. In g_{LR}^{nrs}, however, these parity constraints are reversed. The couplings are related by the equation $g_{RL}^{nrs}=g_{LR}^{srn}$. The modified propagator of a fermionic KK mode n is

$$\frac{1}{\not{p}-m_n-\Sigma_n(\not{p})}$$

where (using Feynman's parametrization and Wick's rotation)

$$-i\Sigma_n(\not{p})=\sum_{r,s}f^2\int^{\Lambda}\frac{d^4k}{(2\pi)^4}\frac{1}{k^2-m_r^2}(g_{RL}^{nrs}P_L$$
$$+g_{LR}^{nrs}P_R)\frac{1}{(\not{p}-\not{k})-m_s}(g_{LR}^{nrs}P_L+g_{RL}^{nrs}P_R)$$
$$\to\frac{if^2}{16\pi^2}\sum_{r,s}\left(\frac{1}{2}[(g_{RL}^{nrs})^2P_R+(g_{LR}^{nrs})^2P_L]\not{p}\right.$$
$$\left.+g_{RL}^{nrs}g_{LR}^{nrs}m_s\right)\ln\left(\frac{\Lambda^2}{m_s^2}\right). \quad (43)$$

[6]For $r\leqslant L<1/M_Z$, one needs to take into account the full electroweak contribution. But if we neglected the contribution from the Z boson and its KK modes as an illustrative computation, we would obtain to leading orders (40) $V(r)\simeq 2e^2L/\pi r^2+\pi e^2/6L-3e^2L/\pi wur^4+\cdots$. It is interesting that, for $r\leqslant L$, the model-independent leading order of the potential is $\sim 1/r^2$, which agrees with the classical result obtained by the Gaussian theorem [1] in a purely geometric approach.

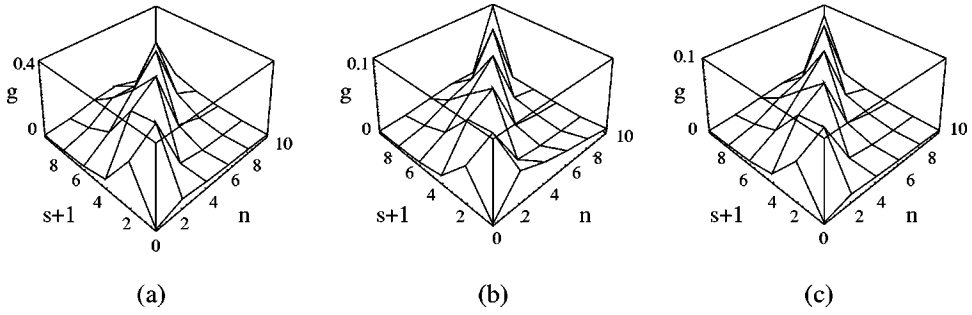

FIG. 6. Coupling $g_{RL}^{\bar{n}rs}$ [Eq. (42)] as a function of n,s with $u=1$, $w/u=10.3$, $uL=40$. The background scalar field $\phi_{\bar{r}}^{-}$ is in the normalizable (bound) KK mode (a), or $\bar{r}=0$ mode (b), or $\bar{r}=5$ mode (c). The position of the peaks clearly indicates $n=s+1$ enhancement. We note also that the last two graphs are very similar, which justifies our approximation leading to Eq. (44).

Λ is a cutoff scale above which the physics is governed by a more fundamental theory, and the sum over KK modes is accordingly limited by the relations $\bar{m}_{\bar{r}}^2, m_s^2 \leqslant \Lambda^2$.

If $\Lambda^2 \geqslant w^2$, heavy KK modes ($\bar{m}_{\bar{r}}^2 \geqslant u^2, m_s^2 \geqslant w^2$) will contribute to the sum (43) and drive its value to that of the UED scenario. In this work we assume $\Lambda^2 \leqslant w^2$ to investigate the contribution, if any, solely from the distinctive lower part of the KK spectrum of the brane picture. This assumption is self-consistent because by tuning u and w we can push Λ to a sufficiently high scale, and the nonrenormalizable contribution is expected to be cutoff by quantum gravitational effects [10]. With this assumption, from the orbifolding constraints (34) and (35), it follows that only the lower KK scalar modes ($\bar{r} \ll uL$) appear in the sum (43) as their masses are below the cutoff. The number of these relevant modes is $N_s \sim \mathcal{O}(1)$ in the limit $L \gg 1/u$ considered here. This observation allows a rough evaluation of the nonuniversal couplings $g_{RL}^{\bar{n}rs}$.

Specific solutions of $\xi_{nR,L}$ [Eqs. (A9), (A23)] and $f_{\bar{r}}^{-}$[Eqs. (A33), (A40)] suggest that for KK modes relevant to the self-energy diagram ($n,s \leqslant w/u; \bar{r} \ll uL$), the characteristic width of the normalized wave function of the KK fermion $\xi_{nR,L}(y)$ in the extra dimension is much smaller than that of $f_{\bar{r}}^{-}(y)$ (of the scalar field) as w is sufficiently larger than u.[7] For a rough estimation we neglect the variation of $f_{\bar{r}}^{-}(y)$ over the extent of $\xi_{nR,L}(y)$; then for each relevant mode $\bar{r}$ the couplings $g_{RL}^{\bar{n}rs}$ are most enhanced for a few modes s closest to n (i.e., when $n \simeq s+1$), because this is when ξ_{nR} resembles ξ_{sL} most closely (i.e., $2\int_0^L \xi_{nR}\xi_{sL}dy \sim 1$). In this approximation, the fermionic KK zero-mode mass should receive a rather small one-loop correction, because it has no corresponding "closest-neighbor" mode ξ_{sL} with $s=-1$, i.e., $g_{RL}^{\bar{0}r-1} = g_{LR}^{\bar{-1}r0} = 0$. Our estimation is verified by a particular numerical evaluation of the coupling $g_{RL}^{\bar{n}rs}$ as a function of the mode indices n,s. The result is presented in Fig. 6, where one can see clearly the effect of closest-neighbor enhancement on the values of the couplings. The values of these couplings indeed decrease very quickly off the diagonal $n=s+1$. Putting all observations together, for the KK nonzero mode of the fermion we have

$$-i\Sigma_n(\not{p}) = \mathcal{C}\frac{i}{16\pi^2}\frac{f^2}{2L}\ln\left(\frac{\Lambda^2}{m_n^2}\right)\left(\frac{1}{2}\not{p} + m_n\right), \qquad (44)$$

where $\mathcal{C} \sim \mathcal{O}(1)$ accounts for the number of relevant KK scalar modes in the sum and some crude estimations that we have made. This one-loop divergence requires the corresponding counterterms

$$\mathcal{L} \to \mathcal{L} + \delta\mathcal{L} = \sum_n \left(Z_\psi \bar{\psi}_n i\not{\partial}\psi_n - Z_m m_n \bar{\psi}_n \psi_n\right)$$

with renormalization scaling factors

$$Z_\psi = 1 - \frac{\mathcal{C}}{64\pi^2}\frac{f^2}{2L}\ln\left(\frac{\Lambda^2}{m_n^2}\right),$$

$$Z_m = 1 + \frac{\mathcal{C}}{32\pi^2}\frac{f^2}{2L}\ln\left(\frac{\Lambda^2}{m_n^2}\right).$$

After transforming to the canonical basis $\psi \to \sqrt{Z_\psi}\psi$ we finally obtain a one-loop correction to the mass of the fermionic KK nonzero mode (in the leading order):

$$\delta m_n = m_n\left(\frac{Z_\psi}{Z_m} - 1\right) \simeq m_n\left(\frac{3\mathcal{C}}{64\pi^2}\frac{f^2}{2L}\ln\frac{\Lambda^2}{m_n^2}\right), \qquad (45)$$

where the m_n's are given by Eq. (16). Interestingly, the same result is obtained in [11], where the one-loop correction to the KK mass in the UED scenario was computed using a fundamental 5D approach (see [12]). This would indicate that, at the tree level, KK mass structures in the fat brane and UED scenarios are very different at least in the lower part, as we saw in previous sections; however, their radiative corrections may scale somewhat similarly. We now turn to some resonant effects on the KK spectrum of fermions.

[7]This assertion can be less rigorous for KK modes $s \to w/u$ in the upper limit of the sum, but contributions from these modes are actually suppressed by the factor $\ln(\Lambda/m_s)$.

V. RESONANCES AND KALUZA-KLEIN SPECTRUM OF FERMIONS

The considerations of Sec. III led to the conclusion that orbifold boundary conditions, which are crucial ingredients in achieving single-chirality standard model fermions as zero modes of fields in a higher-dimensional theory, act to suppress many bound ($m^2<w^2$) fermionic KK levels. Each of these levels' wave functions has a definite parity with respect to a fixed point, and if this parity is not identical to the one imposed by OBCs, the corresponding level is suppressed by parity mismatch. Higher levels ($m^2\geqslant w^2$) are twofold degenerate and can be arranged to have the desired parities (see the Appendix), so the impact of OBCs on these levels is not so obvious. In this section we discuss in more detail the structure of this upper part of the KK spectrum and clarify the close connection between periodic boundary conditions, orbifold boundary conditions, and the complex transmission amplitude of free fermions through the double-brane system mentioned in Sec. III.

We first consider the related problem of one noncompact dimension where a fermion, being free at infinity, approaches a single double-well potential $V_R^{(2)}$ [Eq. (28)] (Fig. 2) with wave vector $ku\equiv\sqrt{m^2-w^2}>0$. In this problem, the wave function of the particle is not constrained by any boundary conditions since the dimension is noncompact. The most general particle wave function and its asymptotic forms as referred to the fixed point at $y=0$ are, respectively [see Eqs. (A12), (A13)],

$$\xi_{mR}(y)=aR_1(y)+bR_2(y), \tag{46}$$

$$y\to\infty:\ \xi_{mR}(y)\to ae^{ikuy}+be^{-ikuy}, \tag{47}$$

$$y\to-\infty:\ \xi_{mR}(y)\to(aC_1+bC_2)e^{-ikuy}+(aD_1+bD_2)e^{ikuy}. \tag{48}$$

As referred to the fixed point at $y=L$, similarly we have

$$\xi'_{mR}(y)=a'L_1(y')+b'L_2(y'), \tag{49}$$

$$y'\to\infty:\ \xi'_{mR}(y)\to a'e^{ikuy'}+b'e^{-ikuy'}, \tag{50}$$

$$y'\to-\infty:\ \xi'_{mR}(y)\to(a'C'_1+b'C'_2)e^{-ikuy'}+(a'D'_1+b'D'_2)e^{ikuy'}, \tag{51}$$

where $y'=y-L$ and a,b,a',b' are constant coefficients.

For the wave traveling from left to right and scattering on the double brane, we let $b'=0$ and the matching of Eqs. (47) and (51) gives $a/b=(D'_1/C'_1)\exp(-2ikuL)$ and $a'/b=1/C'_1$. Next, using the relations (A18) $C_1=-D_2$, $C_2=D_1^*$, and $D'_2=-D_2=D_2^*$, we obtain the transmission amplitude

$$t_R=\frac{a'}{aD_1+bD_2}=\frac{1}{D_1D'_1\exp(-2ikuL)+D_2^2}. \tag{52}$$

Now we see clearly that conditions (30), (31) imply the physical requirement that the complex transmission amplitude of a fermion propagating through a single double-well potential $V_R^{(2)}$ is precisely 1. We will come back to this observation below. A similar consideration gives an identical transmission amplitude for a wave function subject to the other type of single double-well potential $V_L^{(2)}$ [Eq. (28)]: $t_L=t_R$. From here on we drop all indices R,L as well as the factor $\exp(-2ikuL)$ in the expression of t by virtue of Eq. (30).

For $k\gg w/u>1$, we saw earlier that $m_n^2\simeq n^2\pi^2/L^2$, i.e., the higher KK structure is always dominated by the usual periodic compactification. Now we can see this result more physically: the high-lying KK modes have a large transmission amplitude $t\to1$ because they are not sensitive to the underlying potential and can cross it without significant reflection, and on these modes, the periodic boundary conditions (30) are the more influential ones. However, as seen in the previous section, the couplings f and λ in Eq. (3) have negative dimensions of mass, so the theory is not renormalizable. It may effectively describe physics only under a certain mass scale, and our calculation may no longer be relevant for heavy KK modes above that scale. Apart from this, the smaller range of values of k deserves special interest also because it is where the fat brane structure is expected to play a dominant role. To see this specifically, we now examine the mass quantization equation $t=1$ [Eq. (31)] for low-lying fermionic KK states, $k\ll1<w/u$. Using the product expansion [13]

$$\frac{\Gamma(z_1)\Gamma(z_2)}{\Gamma(z_1+z_3)\Gamma(z_2-z_3)}=\prod_{q=0}^{\infty}\left(1+\frac{z_3}{z_1+q}\right)\left(1-\frac{z_3}{z_2+q}\right)$$

we can expand D_1 as follows:

$$\begin{aligned}D_1&=\frac{k-iw/u}{k}\prod_{q=1}^{\infty}\left(1-\frac{w/u}{q-ik}\right)\left(1+\frac{w/u}{q-ik}\right)\\&=|D_1|\exp\left\{-i\frac{\pi}{2}+i\left[\frac{w}{u}\right]\pi+ik\frac{u}{w}+ik\sum_{q=1}^{\infty}\left(\frac{2}{q}-\frac{1}{q-w/u}-\frac{1}{q+w/u}\right)+\mathcal{O}(k^3)\right\}\\&=|D_1|\exp\left\{-i\frac{\pi}{2}+i\left[\frac{w}{u}\right]\pi+ik\frac{u}{w}+ik\left[2\gamma+\Psi\left(\frac{w}{u}\right)+\Psi\left(\frac{-w}{u}\right)\right]+\mathcal{O}(k^3)\right\}\end{aligned}$$

where $[w/u]$ is the maximal integer not larger than w/u, $\Psi(z)\equiv(d/dz)\ln\Gamma(z)$ is the PolyGamma function, and $\gamma\approx0.577$ is the Euler-Mascheroni constant. After expanding D'_1 in a similar way and using the recursion formula $\Psi(s+1)=\Psi(s)+1/s$ we obtain

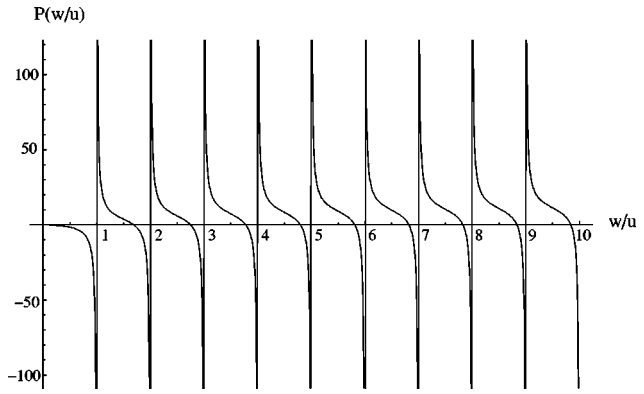

FIG. 7. Sketch of function $P(w/u) \equiv 2[2\gamma + \Psi(w/u) + \Psi(-w/u)]$.

$$D_1 D_1' = |D_1 D_1'| \exp\left[ikP\left(\frac{w}{u}\right) + \mathcal{O}(k^3)\right] = |D_1^2| \exp\left[ikP\left(\frac{w}{u}\right) + \mathcal{O}(k^3)\right] \tag{53}$$

with

$$P\left(\frac{w}{u}\right) \equiv 2\left[2\gamma + \Psi\left(\frac{w}{u}\right) + \Psi\left(\frac{-w}{u}\right)\right]. \tag{54}$$

Now putting this back into the expression (52) of the transmission amplitude, we find

$$t = \frac{1}{D_1 D_1' + D_2^2} = \frac{1}{|D_1|^2 \exp[ikP(w/u) + \mathcal{O}(k^3)] - |D_2|^2} \tag{55}$$

where $|D_1|^2, |D_2|^2$ are calculated in the Appendix:

$$|D_1|^2 = \frac{\sinh^2 \pi k + \sin^2 \pi w/u}{\sinh^2 \pi k}, \quad |D_2|^2 = \frac{\sin^2 \pi w/u}{\sinh^2 \pi k}. \tag{56}$$

First, if w/u has values such that $P(w/u)$ in Eq. (54) or $(\sin^2 \pi w/u)$ in Eq. (56) vanishes, one can see that $t = 1 + \mathcal{O}(k)$, i.e., the condition (31) is approximately satisfied for low-lying KK modes $k \ll 1$. Using the condition (30), this means $n \ll uL$, and since we are considering the limit $uL \gg 1$, this approximation holds for a certain number of modes. This again can be seen as a resonance behavior of the potentials (28) such that for certain values of w/u, even low-lying particles can essentially go through it, and the condition (30) then determines their masses $m_n^2 \approx w^2 + n^2 \pi^2 / L^2$. The resonance values of w/u are positive integers [for $\sin(\pi w/u) = 0$] and others that are solutions of the equation $P(w/u) = 0$. From Fig. 7 we see that there is exactly one such solution between any two successive integers. For all other values of w/u, we find that $t = \mathcal{O}(k)$ and the equation $t = 1$ does not have solutions for $k \ll 1$. In other words, branes are almost "opaque" for low-lying modes and consequently these fermion modes are absent in the KK spectrum.

Overall, except for some particular values of the bulk potential parameter w/u, we see that the lower part of the KK spectrum of fermions is strongly distorted (i.e., suppressed) by orbifold compactification and the VEV of the background scalar field.

VI. CONCLUSION

In this work we attempt to investigate the effect of finite size of the extra dimension (and of the brane) on the KK mode structure of fermions and scalar fields by invoking the analogous bulk potential. The orbifold compactification of the extra dimension involves different types of boundary conditions: the usual periodic boundary conditions dominate the high-lying KK modes and give them the familiar structure of conventional compactification, the orbifold boundary conditions (along with nontrivial fat branes) dominate the bound and low-lying KK modes and give them a more distinctive structure. The observation being emphasized here is that these conditions on wave functions are not always compatible, depending on the specific values of the parameters of the model through some resonance effects. Roughly speaking, the limit separating the two very different parts of the spectrum is of the order of the potential barrier's height experienced by particles along the extra dimension, and this could serve as the cutoff scale of the nonrenormalizable higher-dimensional theory. The effects of orbifold compactification and symmetry breaking in the transverse dimension are now embedded in the 4D effective couplings, and the corresponding vertex interactions do not necessarily conserve the KK number. This allows KK modes to contribute to tree- and higher-level processes. For an extra dimension of arbitrary size, certain numerical techniques are required to solve for the background scalar VEV subject to given orbifold boundary conditions. The matching of component wave functions is not simple, but we believe that the use of the bulk potential would remain the right approach to find the KK masses and their state functions in this general case.

ACKNOWLEDGMENTS

P.Q.H. would like to thank Gino Isidori and the Theory Group at LNF (Frascati) for hospitality during the course of this work. N.-K.T. would like to thank Dr. A. Soddu, Professor V. Celli, and Professor P. Arnold for many helpful discussions and advice. This work is supported in part by the U.S. Department of Energy under Grant No. DE-A505-89ER40518.

APPENDIX

In this appendix, we solve and classify the different solutions of the differential Eqs. (14), which have been accordingly employed with different physical constraints in the main text. First, let us introduce some shorthand notation,

$$w \equiv fv, \quad u \equiv \sqrt{\frac{\lambda v^2}{2}}, \quad z \equiv \tanh\sqrt{\frac{\lambda v^2}{2}}\, y = \tanh uy,$$

$$\varepsilon \equiv \sqrt{\frac{w^2-m^2}{u^2}}. \tag{A1}$$

Dividing both sides of the first equation in (14) by $u^2(1-z^2)$, we obtain

$$\frac{d}{dz}\left((1-z^2)\frac{d\xi_{mR}}{dz}\right)+\left[\frac{w}{u}\left(\frac{w}{u}+1\right)-\varepsilon^2\frac{1}{1-z^2}\right]\xi_{mR}=0. \tag{A2}$$

Again, using some new notation, $z_1 \equiv \frac{1}{2}(1-z)$ and $\xi_{mR}(z) \equiv (1-z^2)^{\varepsilon/2}p(z)$ we transform Eq. (A2) into the standard hypergeometric differential equation

$$z_1(1-z_1)\frac{d^2p}{dz_1^2}+(\varepsilon+1)(1-2z_1)\frac{dp}{dz_1} -\left(\varepsilon-\frac{w}{u}\right)\left(\varepsilon+\frac{w}{u}+1\right)p=0. \tag{A3}$$

Equation (A3) has two linearly independent solutions [13]

$$r_1(z_1)=F\left(\varepsilon-\frac{w}{u},\varepsilon+\frac{w}{u}+1,\varepsilon+1;z_1\right)$$

$$r_2(z_1)=z_1^{-\varepsilon}F\left(-\frac{w}{u},\frac{w}{u}+1,-\varepsilon+1;z_1\right),$$

where F is the hypergeometric function

$$F(a,b,c;z)=1+\frac{ab}{c}\frac{z}{1!}+\frac{a(a+1)b(b+1)}{c(c+1)}\frac{z^2}{2!}+\cdots. \tag{A4}$$

Two corresponding solutions of Eq. (A2) are

$$R_1(y)=(1-z^2)^{\varepsilon/2}r_1(z) =\left(\frac{1}{\cosh uy}\right)^{\varepsilon}F\left(\varepsilon-\frac{w}{u},\varepsilon+\frac{w}{u}+1,\varepsilon+1;\frac{1}{1+e^{2uy}}\right), \tag{A5}$$

$$R_2(y)=(1-z^2)^{\varepsilon/2}r_1(z) =(2e^{uy})^{\varepsilon}F\left(-\frac{w}{u},\frac{w}{u}+1,-\varepsilon+1;\frac{1}{1+e^{2uy}}\right). \tag{A6}$$

First, consider the discrete spectrum $m^2<w^2$; $\varepsilon>0$. The asymptotic forms of Eqs. (A5), (A6) are

$$y\to\infty: \quad R_1(y)\to 2^{\varepsilon}e^{-\varepsilon uy},$$

$$y\to-\infty: \quad R_1(y)\to 2^{\varepsilon}e^{\varepsilon uy}F\left(\varepsilon-\frac{w}{u},\varepsilon+\frac{w}{u}+1,\varepsilon+1;1\right), \tag{A7}$$

$$y\to\infty: \quad R_2(y)\to 2^{\varepsilon}e^{\varepsilon uy},$$

$$y\to-\infty: \quad R_2(y)\to 2^{\varepsilon}e^{\varepsilon uy}F\left(-\frac{w}{u},\frac{w}{u}+1,-\varepsilon+1;1\right). \tag{A8}$$

When $L\to\infty$ as considered in Sec. II, we see from Eq. (A8) that R_2 blows up at infinity and cannot be a physical solution for bound states, and

$$\xi_{mR}(y)=R_1(y) =\left(\frac{1}{\cosh uy}\right)^{\varepsilon}F\left(\varepsilon-\frac{w}{u},\varepsilon+\frac{w}{u}+1,\varepsilon+1;\frac{1}{1+e^{2uy}}\right) \tag{A9}$$

is the sought physical solution of ξ_{mR} with the following condition [otherwise, F in Eq. (A7) and then ξ_{mR} in Eq. (A9) blows up as $y\to-\infty$]:

$$\varepsilon-\frac{w}{u}=-n_R \quad (n_R\in N). \tag{A10}$$

From this follows the mass quantization of KK discrete levels [Eq. (16)]. As far as the zero mode ($m=0$) is concerned, in some computations it is more convenient to approximate ξ_{0R} with a normalized Gaussian function

$$\xi_{0R}(y)=\left(\frac{wu}{\pi}\right)^{1/4}e^{-wuy^2/2}. \tag{A11}$$

The fact that here only R_1 is a physical solution is readily understood, as all bound states of a 1D potential are nondegenerate. Further, we see from Eq. (A9) that ξ_{mR} is an even or odd function, respectively, when n_R is an even or odd integer. For the continuous spectrum, $m^2\geqslant w^2$, $k \equiv \sqrt{(m^2-w^2)/u^2}=i\varepsilon$, Eqs. (A5), (A6) read

$$R_1(y)=\left(\frac{1}{\cosh uy}\right)^{-ik}F\left(-ik-\frac{w}{u}, -ik+\frac{w}{u}+1,-ik+1;\frac{1}{1+e^{2uy}}\right), \tag{A12}$$

$$R_2(y)=(2e^{uy})^{-ik}F\left(-\frac{w}{u},\frac{w}{u}+1,ik+1;\frac{1}{1+e^{2uy}}\right), \tag{A13}$$

whose asymptotic forms are

$$y\to\infty:\ \ R_1(y)\to 2^{-ik}e^{iuy},$$

$$y\to-\infty:\ \ R_1(y)\to 2^{-ik}(C_1e^{-iuy}+D_1e^{iuy}), \tag{A14}$$

$$y\to\infty:\ \ R_2(y)\to 2^{-ik}e^{-iuy},$$

$$y\to-\infty:\ \ R_2(y)\to 2^{-ik}(C_2e^{-iuy}+D_2e^{iuy}), \tag{A15}$$

where for the limit $y\to-\infty$, we have used a fundamental analytic continuation formula of the hypergeometric function [13]

$$F(a,b,c;z)=\frac{\Gamma(c)\Gamma(c-a-b)}{\Gamma(c-a)\Gamma(c-b)}F(a,b,a+b+1-c;1-z)+(1-z)^{c-a-b}\frac{\Gamma(c)\Gamma(a+b-c)}{\Gamma(a)\Gamma(b)}\times F(c-a,c-b,c+1-a-b;1-z) \tag{A16}$$

and

$$C_1=\frac{\Gamma(ik)\Gamma(1-ik)}{\Gamma(w/u+1)\Gamma(-w/u)},$$

$$D_1=\frac{\Gamma(-ik)\Gamma(1-ik)}{\Gamma(-ik-w/u)\Gamma(-ik+w/u+1)},$$

$$C_2=\frac{\Gamma(ik)\Gamma(1+ik)}{\Gamma(ik-w/u)\Gamma(ik+w/u+1)},$$

$$D_2=\frac{\Gamma(-ik)\Gamma(1+ik)}{\Gamma(w/u+1)\Gamma(-w/u)}. \tag{A17}$$

Using the Gamma function relations [14] $\Gamma(z+1)=z\Gamma(z)$, $\Gamma(z)\Gamma(1-z)=\pi/\sin(\pi z)$, we obtain some relations useful for our calculation:

$$C_1=\frac{i\sin\pi w/u}{\sinh\pi k}\Rightarrow|C_1|^2=\frac{\sin^2\pi w/u}{\sinh^2\pi k}$$

$$C_1=-D_2,\quad C_2=D_1^*\Rightarrow|C_1|^2=|D_2|^2,$$

$$|C_2|^2=|D_1|^2,$$

$$|D_1|^2-|D_2|^2=|D_1|^2+D_2^2=1\Rightarrow|D_1|^2=\frac{\sinh^2\pi k+\sin^2\pi w/u}{\sinh^2\pi k}. \tag{A18}$$

We note especially that when w/u is integer $D_2=0$ and $|D_1|=1$.

In contrast with bound states, neither of (A12), (A13) has definite parity. However, continuous levels of 1D potential are always two-fold degenerate, so we can linearly combine R_1, R_2 to produce a function of the desired parity. From Eqs. (A14), (A15) we can respectively build up the even and odd right-handed wave functions:

$$R_{even}(y)=R_1(y)+\frac{D_1}{1-D_2}R_2(y), \tag{A19}$$

$$R_{odd}(y)=R_1(y)-\frac{D_1}{1+D_2}R_2(y). \tag{A20}$$

A similar consideration applies to the left-handed fermion wave functions, in place of Eqs. (A5), (A6) we have

$$L_1(y)=\left(\frac{1}{\cosh uy}\right)^{\varepsilon}F\left(\varepsilon-\frac{w}{u}+1,\varepsilon+\frac{w}{u},\varepsilon+1;\frac{1}{1+e^{2uy}}\right), \tag{A21}$$

$$L_2(y)=(2e^{uy})^{\varepsilon}F\left(-\frac{w}{u}+1,\frac{w}{u},-\varepsilon+1;\frac{1}{1+e^{2uy}}\right). \tag{A22}$$

The key observation here, when comparing Eqs. (A5), (A6) with Eqs. (A21), (A22), is that left-handed solutions L_1,L_2 are effectively the same as R_1,R_2 after changing w/u to $w/u-1$. Then the corresponding physical solutions and mass quantization equation for a left-handed discrete spectrum are [see Eqs. (A9), (A7), (A10)]

$$\xi_{mL}(y)=L_1(y)=\left(\frac{1}{\cosh uy}\right)^{\varepsilon}\times F\left(\varepsilon-\frac{w}{u}+1,\varepsilon+\frac{w}{u},\varepsilon+1;\frac{1}{1+e^{2uy}}\right) \tag{A23}$$

$$y\to\infty:\quad L_1(y)\to 2^{\varepsilon}e^{-\varepsilon uy}, \tag{A24}$$

$$\varepsilon-\frac{w}{u}+1=-n_L(n_L\in N). \tag{A25}$$

In the continuous spectrum, instead of Eqs. (A12)–(A15), we have

$$L_1(y)=\left(\frac{1}{\cosh uy}\right)^{-ik}F\left(-ik-\frac{w}{u}+1,-ik+\frac{w}{u},-ik+1;\frac{1}{1+e^{2uy}}\right), \tag{A26}$$

$$L_2(y)=(2e^{uy})^{-ik}F\left(-\frac{w}{u}+1,\frac{w}{u},ik+1;\frac{1}{1+e^{2uy}}\right), \tag{A27}$$

$$y\to\infty:\quad L_1(y)\to 2^{-ik}e^{iku y},$$

$$y\to-\infty:\quad L_1(y)\to 2^{-ik}(C_1' e^{-iku y}+D_1' e^{iku y}), \tag{A28}$$

$$y\to\infty:\quad L_2(y)\to 2^{-ik}e^{-iku y},$$

$$y\to-\infty:\quad L_2(y)\to 2^{-ik}(C_2' e^{-iku y}+D_2' e^{iku y}), \tag{A29}$$

where

$$C_1'=\frac{\Gamma(ik)\Gamma(1-ik)}{\Gamma(w/u)\Gamma(-w/u+1)},\quad D_1'=\frac{\Gamma(-ik)\Gamma(1-ik)}{\Gamma(-ik-w/u+1)\Gamma(-ik+w/u)},$$

$$C_2'=\frac{\Gamma(ik)\Gamma(1+ik)}{\Gamma(ik-w/u+1)\Gamma(ik+w/u)},\quad D_2'=\frac{\Gamma(-ik)\Gamma(1+ik)}{\Gamma(w/u)\Gamma(-w/u+1)}. \tag{A30}$$

By making the change $w/u\to w/u-1$ in Eq. (A18) we can find similar properties of C_1', C_2', D_1', D_2'. In particular, we have $D_2'=-D_2$, $|D_1'|=|D_1|$. The even and odd left-handed wave functions now are

$$L_{even}(y)=L_1(y)+\frac{D_1'}{1-D_2'}L_2(y), \tag{A31}$$

$$L_{odd}(y)=L_1(y)-\frac{D_1'}{1+D_2'}L_2(y). \tag{A32}$$

Finally, for a scalar field, Eq. (22) can be solved by the same method. For a discrete spectrum, $\bar{m}^2<4u^2$, $\bar{\varepsilon}\equiv\sqrt{(4u^2-\bar{m}^2)/u^2}>0$, we obtain, respectively, the scalar wave function and mass quantization equation

$$f_{\bar{n}}(y)=\left(\frac{1}{\cosh uy}\right)^{\bar{\varepsilon}}F\left(\bar{\varepsilon}-2,\bar{\varepsilon}+3,\bar{\varepsilon}+1;\frac{1}{1+e^{2uy}}\right), \tag{A33}$$

$$\bar{\varepsilon}-2=-\bar{n}(\bar{n}\in N). \tag{A34}$$

Since $\bar{\varepsilon}>0$, there are only two discrete levels $\bar{n}=0,1$ and the corresponding states are symmetric and antisymmetric at $y=0$. In the continuous spectrum, $\bar{m}^2\geqslant 4u^2$, $\bar{k}\equiv\sqrt{(\bar{m}^2-4u^2)/u^2}=i\bar{\varepsilon}$, in place of Eqs. (A12)–(A15), (A19), (A20), we have

$$S_1(y)=\left(\frac{1}{\cosh uy}\right)^{-i\bar{k}}F\left(-i\bar{k}-2,-i\bar{k}+3,-i\bar{k}+1;\frac{1}{1+e^{2uy}}\right), \tag{A35}$$

$$S_2(y)=(2e^{uy})^{-i\bar{k}}F\left(-2,3,i\bar{k}+1;\frac{1}{1+e^{2uy}}\right) \tag{A36}$$

$$y\to\infty:\quad S_1(y)\to 2^{-i\bar{k}}e^{i\bar{k}uy},$$

$$y\to-\infty:\quad S_1(y)\to 2^{-i\bar{k}}(\bar{D}e^{i\bar{k}uy}), \tag{A37}$$

$$y\to\infty:\quad S_2(y)\to 2^{-i\bar{k}}e^{-i\bar{k}uy},$$

$$y\to-\infty:\quad S_2(y)\to 2^{-i\bar{k}}\left(\frac{1}{\bar{D}}e^{-iku y}\right), \tag{A38}$$

$$S_{even}(y)=S_1(y)+\bar{D}S_2(y), \tag{A39}$$

$$S_{odd}(y)=S_1(y)-\bar{D}S_2(y), \tag{A40}$$

where

$$\bar{D}=\frac{\Gamma(-i\bar{k})\Gamma(1-i\bar{k})}{\Gamma(-i\bar{k}-2)\Gamma(-i\bar{k}+3)}=\frac{(1+i\bar{k})(2+i\bar{k})}{(1-i\bar{k})(2-i\bar{k})}. \tag{A41}$$

[1] I. Antoniadis, Phys. Lett. B **246**, 377 (1990); N. Arkani-Hamed, S. Dimopoulos, and G. Dvali, *ibid.* **429**, 263 (1998); I. Antoniadis, N. Arkani-Hamed, S. Dimopoulos, and G. Dvali, *ibid.* **436**, 257 (1998).

[2] N. Arkani-Hamed and M. Schmaltz, Phys. Rev. D **61**, 033005 (2000).

[3] R. Jackiw and C. Rebbi, Phys. Rev. D **13**, 3398 (1976).

[4] H. Georgi, A.K. Grant, and G. Hailu, Phys. Rev. D **63**, 064027 (2001).

[5] D.E. Kaplan and T.M. Tait, J. High Energy Phys. **11**, 051 (2001).

[6] L. D. Landau and E. M. Lifshitz, *Quantum Mechanics*, 3rd ed. (Pergamon Press, Oxford, 1977).

[7] E.A. Mirabelli and M. Schmaltz, Phys. Rev. D **61**, 113011 (2000); G.C. Branco, A. de Gouvea, and M.N. Rebelo, Phys. Lett. B **506**, 115 (2001); W.F. Chang and J.N. Ng, J. High

Energy Phys. **12**, 077 (2002); Y. Grossman and G. Perez, Phys. Rev. D **67**, 015011 (2003); P.Q. Hung and M. Seco, Nucl. Phys. **B653**, 123 (2003); P.Q. Hung, Phys. Rev. D **67**, 095011 (2003); A. Masiero, M. Peloso, L. Sorbo, and R. Tabbash, *ibid.* **62**, 063515 (2000); A. Soddu and N-K. Tran, *ibid.* **69**, 015010 (2004).

[8] L. Randall and R. Sundrum, Phys. Rev. Lett. **83**, 4690 (1999).

[9] M. Voloshin, Sov. J. Nucl. Phys. **21**, 687 (1975).

[10] T. Appelquist, H.C. Cheng, and B.A. Dobrescu, Phys. Rev. D **64**, 035002 (2001); H.C. Cheng, B.A. Dobrescu, and C.T. Hill, Nucl. Phys. **B589**, 249 (2000).

[11] H.C. Cheng, K.T. Matchev, and M. Schmaltz, Phys. Rev. D **66**, 036005 (2002).

[12] H. Georgi, A.K. Grant, and G. Hailu, Phys. Lett. B **506**, 207 (2001).

[13] A. Erdelyi *et al.*, *Higher Transcendental Functions*, Vol. 1 (McGraw-Hill, New York, 1953).

[14] I. S. Gradshteyn and I. M. Ryznik, *Tables of Integrals, Series, and Products*, 5th ed. (Academic Press, Boston, 1994).